Nevada Bureau of Mines and Geology Special Publication 36

Global Positioning System Constraints on Crustal Deformation Before and During the 21 February 2008 Wells, Nevada M 6.0 Earthquake

by

William C. Hammond[1], Geoffrey Blewitt[1], Corné Kreemer[1],
Jessica R. Murray-Moraleda[2], Jerry L. Svarc[2]
[1]Nevada Bureau of Mines and Geology, University of Nevada, Reno
[2]U.S. Geological Survey, Menlo Park, California

2011

ABSTRACT

Using Global Positioning System (GPS) data from permanent sites and U.S. Geological Survey (USGS) campaign data we have estimated co-seismic displacements and secular background crustal deformation patterns associated with the 21 February 2008 Wells Nevada earthquake. Estimated displacements at nearby permanent GPS sites ELKO (84 km distant) and GOSH (81 km distant) are 1.0±0.2 mm and 1.1±0.3 mm, respectively. The magnitude and direction are in agreement with those predicted from a rupture model based on InSAR measurements of the near-field co-seismic surface displacement. Analysis of long GPS time series (>10 years) from the permanent sites within 250 km of the epicenter indicate the eastern Nevada Basin and Range undergoes steady tectonic transtension with rates on the order of 1 mm/year over approximately 250 km. The azimuth of maximum horizontal crustal extension is consistent with the azimuth of the Wells earthquake co-seismic slip vector. The orientation of crustal shear is consistent with deformation associated with Pacific/North America plate boundary relative motion seen elsewhere in the Basin and Range. In response to the event, we deployed a new GPS site with the capability to telemeter high rate, low latency data that will in the future allow for rapid estimation of surface displacement should aftershocks or postseismic deformations occur. We estimated co-seismic displacements using campaign GPS data collected before and after the event, however in most cases their uncertainties were larger than the offsets. Better precision in co-seismic displacement could have been achieved for the campaign sites if they had been surveyed more times or over a longer interval to better estimate their pre-event velocity.

INTRODUCTION

On 21 February 2008, the M_W 6.0 Wells, Nevada earthquake occurred in a relatively remote area in northeast Nevada. The event epicenter was located 10 kilometers northeast of the town of Wells at the intersection of U.S. Interstate Highway 80 and U.S. Highway 93, approximately 50 km west of the Utah border. The location, event mechanism, and the southeast dip of the planar cloud of aftershocks suggest that the event occurred on a southeast dipping normal fault on the east side of the Snake Mountains, beneath Town Creek Flat (Smith and others, 2010; Dreger and others, 2010). While no surface rupture attributable to the earthquake was observed, InSAR measurements precisely map the location of co-seismic subsidence (Amelung and Bell, 2008), which provides additional constraint on the depth, direction and style of co-seismic slip. The event is an example of Basin and Range normal faulting of a magnitude which occurs only rarely, approximately once per decade. Thus the earthquake offers a special opportunity to study the processes involved in developing the characteristic and eponymous topography of the Basin and Range Province.

While remote, the region around Wells lies near the middle of the newly installed EarthScope deployment of seismic and geodetic instrumentation that was designed to investigate the kinematics and dynamics of the western U.S. continental lithosphere. The USArray transportable array (a mobile deployment of hundreds of seismometers in the process of sweeping across North America) happened to be deployed in the vicinity of the earthquake, allowing for excellent resolution of the event mechanism and aftershock sequence (see Smith and others, 2010; Dreger and others, 2010). The

GPS component of EarthScope, the Plate Boundary Observatory (PBO), was near completion with all but a few stations slated for Nevada completed and collecting data continuously. However, by chance the event occurred in an area of relatively sparse GPS coverage compared to the dense coverage near the more highly populated western and eastern edges of the Great Basin, and about 200 km north of the dense profile that spans the province along U.S. Highway 50. Thus, despite its occurrence in the era of EarthScope, the earthquake occurred in an area of relatively sparse permanent GPS coverage, nearly equidistant (about 60 km) from the several nearest stations. USGS campaign stations were near and dense enough to offer a significant constraint on the co-seismic displacement, but generally had not been surveyed enough times before the event to constrain their pre-event velocity with sufficient precision to estimate the co-seismic displacement.

Because of these conditions, the effort to obtain GPS measurements of this event presented a near worst-case scenario for an earthquake of this size in the western United States. Thus the use of satellite-based Synthetic Aperture Radar (InSAR) was critical for resolving the details of surface displacement that occurred during the earthquake (Amelung and Bell, 2008), and adds to the short list of Basin and Range earthquakes that have been geodetically imaged with InSAR. However, by using specialized GPS data processing methods we have been able to detect displacements of magnitude about 1 mm with 0.3 mm precision (about 99% confidence) from the nearest far-field permanent stations. These estimates are broadly consistent with the predictions based on seismic and InSAR measurement of the co-seismic displacements.

The occurrence of this event was surprising to some since it occurred in a part of the province that has been shown in several studies to have among the slowest crustal deformation rates in the Basin and Range (e.g., Thatcher and others, 1999; Bennett and others, 2003; Hammond and Thatcher, 2004; Kreemer and others, 2010). No Quaternary or younger fault had been mapped that would suggest an active range-bounding normal fault system existed on the west side of Town Creek Flat (Henry and Colgan, 2010). However, the broader region is also characterized by the presence of numerous Holocene- and Quaternary-aged Basin and Range-style normal faults, and diffuse seismicity, which are at odds with the assertion that this part of the province behaves rigidly, e.g., similar to the Sierra Nevada/Great Valley microplate. In this report we present a new analysis of over 10 years of data from the permanent GPS stations in the eastern Nevada Basin and Range. These measurements indicate that the province does deform at a very low (yet detectable) rate, and have a style and orientation that are consistent with the Wells earthquake focal mechanism, and consistent with the co-seismic displacements observed with GPS and InSAR. Observations of the earthquake and the crustal strain together indicate that the Basin and Range in northeast Nevada does not behave as a microplate, but as a zone of low rate and diffuse crustal extension.

GPS DATA AND OBSERVATIONS

Co-seismic Displacements at Permanent GPS Sites

GPS data were used to compute the co-seismic displacement of permanent GPS stations within 200 km of the Wells earthquake epicenter. The analysis was based on a subset of solutions that are routinely produced at UNR for about 3,000 permanent GPS stations from around the world. Dual-frequency carrier phase and pseudorange data were first processed to produce daily precise point position (PPP) solutions independently for all stations (Zumberge and others, 1997), using the GIPSY-OASIS II software from the NASA Jet Propulsion Laboratory (JPL), and using precise satellite orbit and clock products available from JPL. These PPP solutions were then further improved by application of the "Ambizap" algorithm developed at UNR to resolve integer carrier phase ambiguities for massive network solutions (Blewitt, 2008).

The daily global network solutions were then based upon a custom regional reference frame ("GB1") aligned to a constant velocity model for a subset of about 40 deep-braced GPS stations around the Great Basin that have been operating for at least 8 years. Alignment of daily solutions in this manner is known as "spatial filtering" (Wdowinski and others, 1997), which for our analysis was designed to eliminate common-mode signals and errors on the spatial scale of the Great Basin . The resulting de-trended time series of daily station positions in the Great Basin typically have an RMS scatter of about 1 mm in the horizontal components, and about 3 mm in the vertical. It is important to note that these time series are the result of operational analysis not specifically tailored to the Wells earthquake; however, the GB1 reference frame with spatial filtering at a scale of about 2000 km is well-suited for the analysis of the Wells earthquake.

By averaging the pre- and post-seismic daily positions during the weeks following the earthquake one should be able to detect sub-millimeter co-seismic displacements with statistical significance. For an M_w 6 earthquake, this implies the possibility to detect co-seismic displacements within about 100 km of the epicenter, depending on the details of the relative geometry of fault slip and station location, and depending on the quality of data from the stations, how well the station is attached to the underlying bedrock (to minimize local hydrological effects), and more generally, how predictable are the motions of the stations.

Table 1: Co-seismic displacements at permanent GPS stations. Normalized residuals are measured displacement minus the model displacement, divided by the uncertainty in measured displacement.

GPS Station	Distance from Epicenter (km)	East Measured (mm)	North Measured (mm)	East Model (mm)	North Model (mm)	Normalized Residual East	Normalized Residual North
CEDA	177	0.15 ± 0.38	-0.37 ± 0.25	0.21	-0.08	-0.2	-1.2
CLOV	66	0.51 ± 0.26	-0.17 ± 0.20	0.21	-0.31	1.2	0.7
ELKO	84	-0.83 ± 0.21	0.49 ± 0.19	-0.47	0.01	-1.7	2.5
GOSH	81	1.01 ± 0.38	-0.43 ± 0.23	0.73	-0.59	0.7	0.7
LACR	78	0.08 ± 0.27	-0.32 ± 0.20	-0.39	0.01	1.7	-1.7
LEWI	188	-0.26 ± 0.38	0.12 ± 0.26	-0.08	0.00	-0.5	0.5
MOIL	67	-0.29 ± 0.25	0.04 ± 0.24	-0.08	0.08	-0.8	-0.2
P007	64	0.39 ± 0.35	0.20 ± 0.29	-0.19	0.12	1.7	0.3
P084	170	0.57 ± 0.35	0.11 ± 0.19	0.22	-0.11	1.0	1.2
P113	153	0.52 ± 0.40	0.22 ± 0.22	0.31	-0.14	0.5	1.6
RUBY	144	-0.06 ± 0.35	-0.18 ± 0.24	0.10	0.00	-0.5	-0.8

Uncertainties are 1σ

For our analysis, we used permanent geodetic-quality stations that are deeply anchored in bedrock and have proven to have predictable motions that can be adequately modeled as a constant velocity over several years. These include stations of the Basin and Range Geodetic Network (BARGEN), which have recently become part of the EarthScope "PBO Nucleus" GPS network. At the time of the earthquake the new PBO stations had only been operating for about 1 year, and so did not at that time have well-determined site velocities. However, we decided to process data from a few PBO stations that were closest to the epicenter, keeping in mind that their results can be expected to have larger error than the BARGEN sites.

From the above considerations, a total of 11 sites (8 BARGEN + 3 PBO) were selected for further analysis of co-seismic displacements. For each station, we fit a constant velocity model using all available data since 1 January 2004 until the epoch of the earthquake, 21 February 2008. This velocity model was then used to de-trend the daily post-seismic solutions starting on 22 February 2008. An average of daily solutions for 30 days following the earthquake was then used to compute the co-seismic displacement. We used the scatter of the de-trended data within ±30 days of the earthquake to compute an empirical estimate of the error in the co-seismic displacements. Table 1 lists for all stations the distance to the epicenter, estimated co-seismic displacements, and estimated one-standard deviation errors. Co-seismic displacements were most statistically significant (> 95% confidence level) for stations ELKO and GOSH, a result that is in accord with the earthquake rupture model (Amelung and Bell, 2008; Smith and others, 2010; Dreger and others, 2010), which predicts the largest displacements to occur southeast and northwest of the epicenter. Table 1 also shows the displacements predicted from the model, and the normalized residual for each station component. With the exception of the north component for ELKO, the differences between data and model are less than twice the standard error. Figure 1 shows a map of the estimated displacements at the sites and modeled station co-seismic displacements on a regular grid to illustrate how the largest displacements tended to occur where no GPS stations were deployed, e.g., near and northeast of the epicenter. Figure 2 shows the time series of the de-trended relative position between ELKO and GOSH. The figure makes clear the about 2 mm relative displacement in the east component, and the approximately 1 mm relative displacement in the north component.

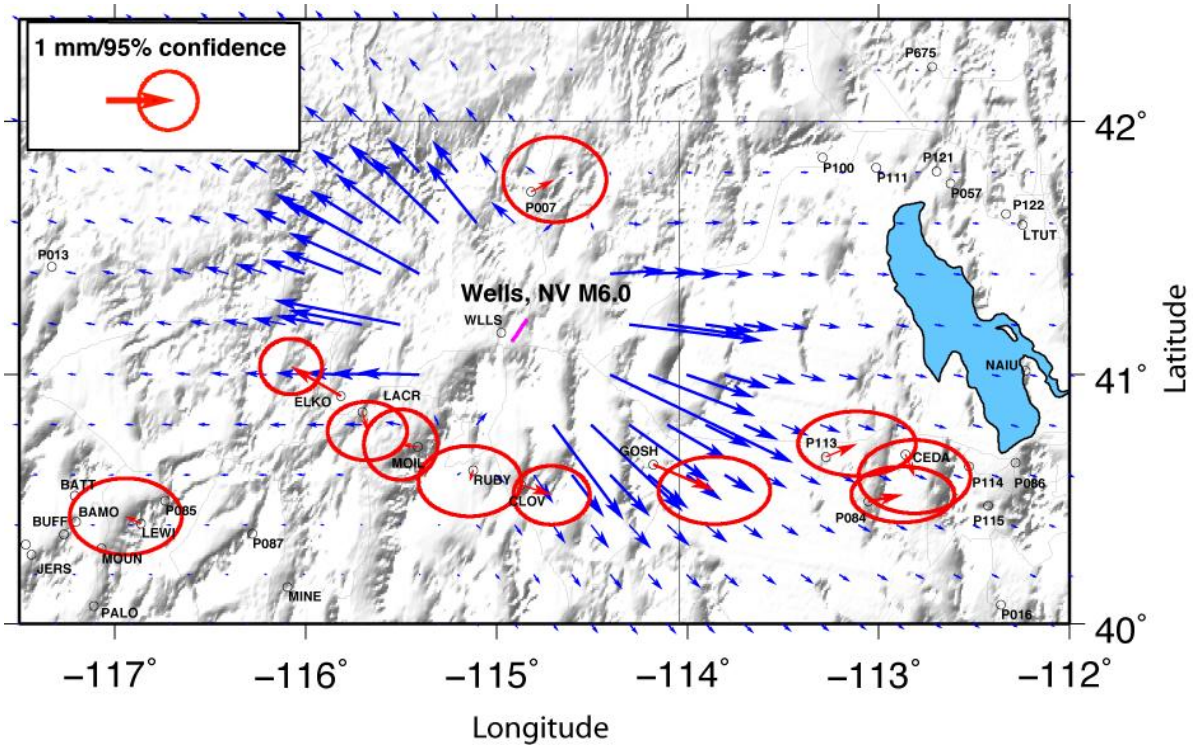

Figure 1. Map of model displacements (blue - Amelung and Bell, 2008), and displacements in GPS time series (red). Maroon line segment is approximate trace of surface projection of model fault plane. Regional permanent GPS sites are shown with black circles. Model displacements within 0.4˚ of epicenter are omitted for clarity.

Secular Tectonic Deformation of the Eastern Nevada Basin and Range

The rate, style, and pattern of background secular crustal deformation of the Basin and Range Province have been studied using geodetic techniques for over three decades (e.g., Savage and others, 1995; Dixon and others, 1995; Wernicke and others, 2000; Dixon and others, 2000; Svarc and others, 2002; Hammond and Thatcher, 2007). This background deformation is usually thought of as the interseismic part of the earthquake cycle that builds the elastic stresses that are episodically released in earthquakes. Thus measurements of interseismic crustal strain can be used to obtain information about earthquakes that occur, or could potentially occur. A consensus has emerged that in the Basin and Range nearly all of the deformation occurs near its eastern and western margins, with the Walker Lane to the west accommodating 7-10 mm/yr, and the Wasatch fault zone to the east accommodating 2-4 mm/yr (Chang and others, 2006; Puskas and others, 2007). The middle longitudes of the province have been thought of as behaving essentially rigidly since deformation measured there was at the time not significantly different from zero (Thatcher and others, 1999; Bennett and others, 2003; Hammond and Thatcher, 2004). As late as 2005, the part of eastern Nevada inside which the Wells earthquake occurred was modeled as a rigid microplate rotating around an Euler pole that lies in southwest Idaho (Hammond and Thatcher, 2005).

Over time our resolution of the deformation of the province has steadily improved. Much of this improvement has come from the proliferation of high-precision GPS measurements at an increased number of sites, but increased precision has also come from the lengthening of GPS time series at the most stable and precisely monumented sites. The BARGEN permanent GPS network was installed in 1996 and early 1997 with deeply braced Wyatt-type monumentation, with approximately 100 km inter-station spacing. These sites now have time series that are over a decade long. The very high precision obtainable with continuously operating GPS sites offers a rare opportunity to study very low rate tectonic deformation.

We have analyzed the seven longest GPS time series of the BARGEN sites that are nearest the epicenter of the Wells earthquake in such a way as to emphasize changes in shape of the network (figure 3). These sites are all south of the earthquake epicenter, but likely represent the state of strain accumulation occurring in the crust around the Wells epicenter prior to the earthquake. Starting with GPS time series in GB1 (discussed above) we applied an additional filtering step using only sites ELKO, RUBY, GOSH, MONI and EGAN in order to remove additional regional common mode noise from the time series. We then computed rates for these sites simultaneously with annual and semi-annual terms in the time series model to minimize bias associated with seasonal variations in GPS positions (although Blewitt and Lavalleé (2002)

found that these biases are very small for time series over several years in length). We then estimated simultaneously from the east and north components of the rates the best horizontal rigid block motion (3 parameters for Euler pole latitude, longitude and rate of rotation) and 3 horizontal strain rates ($\varepsilon_{\theta\theta}$, $\varepsilon_{\phi\phi}$, $\varepsilon_{\theta\phi}$) using the method of Savage and others (2001). The Euler pole parameters were used to calculate the predicted velocities owing to best-fitting rigid-body rotation at each of the GPS sites (red vectors in figure 3), and the rigid rotations were subtracted from the velocities estimated from the GPS data. The resulting rates represent the motion with respect to the local "block", (which is actually not a rigid block but a close approximation). Gradients in these velocities are attributable only to strain inside the eastern Nevada Basin and Range. GPS velocities with gradients associated with rigid body rotation removed are shown in figure 4. The residual velocities (magenta vectors in figure 3) are consistent with the strain rate solution that indicates the direction of maximum extension is N59˚W at a rate of 4.6±0.8 nanostrain/year (nanostrains are 1 part per billion, extension reckoned positive). The direction of maximum horizontal contraction is N31˚E at a rate of 2.8±1.1 nanostrain/year. To estimate the uncertainty in strain rate we scaled the formal uncertainty by the root mean square of the residual misfit of the GPS velocities to the 6-parameter constant strain rate model.

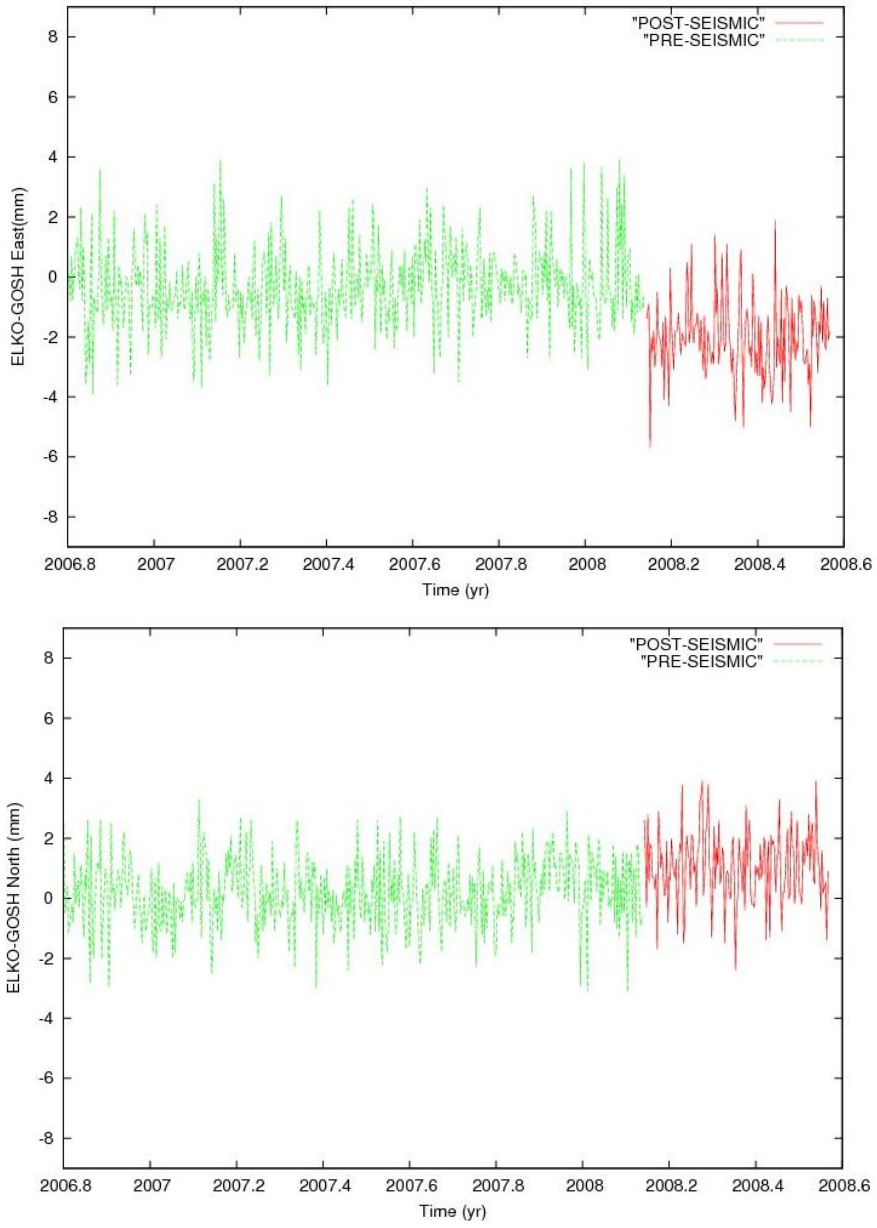

Figure 2. De-trended time series of GPS estimates of relative position between ELKO and GOSH: (top) east component, and (bottom) north component. Green indicates pre-seismic data, and red indicates post-seismic data.

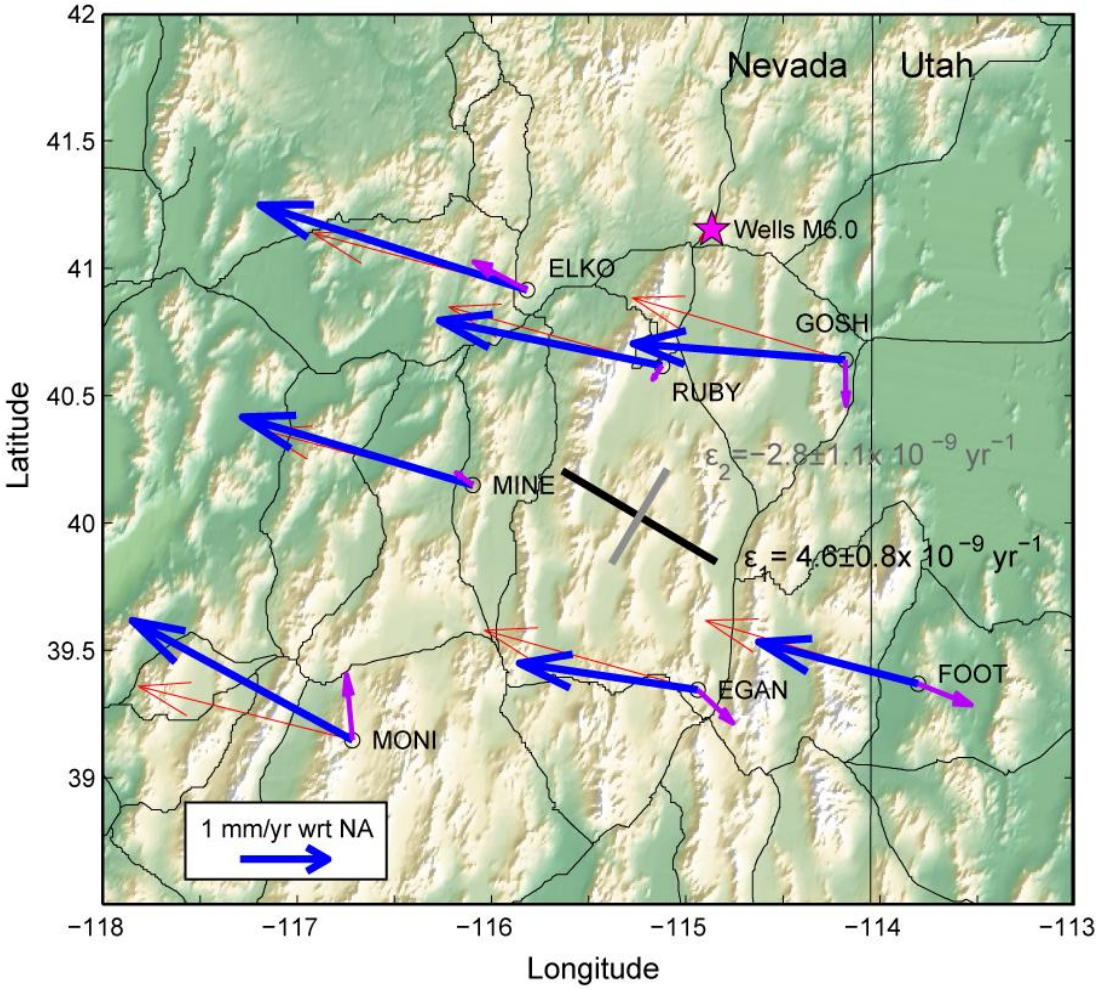

Figure 3. Background secular velocities of BARGEN/PBO permanent GPS sites in vicinity of Wells earthquake with respect to stable North America (blue). Velocities attributable to deformation (magenta) have been inferred by subtracting the best-fitting model of rigid rotation for these sites (red). This network is approximately 250 km wide and experiences horizontal extension with azimuth N59˚W (black tensor strain rate bar), and horizontal contraction N31˚E (gray tensor strain rate bar). Location of Wells earthquake is shown with magenta star.

USGS Campaign GPS Measurements

The U.S. Geological Survey routinely conducts repeated GPS surveys of geodetic markers throughout the western United States using dual-frequency geodetic GPS receivers. Mobile campaign-based surveys require less up-front investment than permanently monumented and telemetered GPS systems, and hence have achieved a broad and dense spatial coverage in Nevada, especially along U.S. Highway 50 and Interstate 80. The greater flexibility and mobility comes at the cost of greater uncertainties in individual daily position solutions. These uncertainties can arise because of 1) error in manually centering the antenna above the monument, 2) error due to change in ground reflections of the GPS signal (multipath) as the antenna is positioned at different heights above the ground each time the tripod is set up, 3) error due to movement of the tripod during each campaign, e.g., due to tripod settling, ground moisture, freeze-thaw, or heavy winds, 4) monument stability, and 5) the practice of collecting data in sessions sometimes shorter than 24 hours. Hence noise in individual positions is larger than for permanent sites, and uncertainties are usually near 3-7 mm in the horizontal and about three times that in the vertical (Hammond, 2004). These uncertainties are about three times greater than for the continuously recording sites reported above.

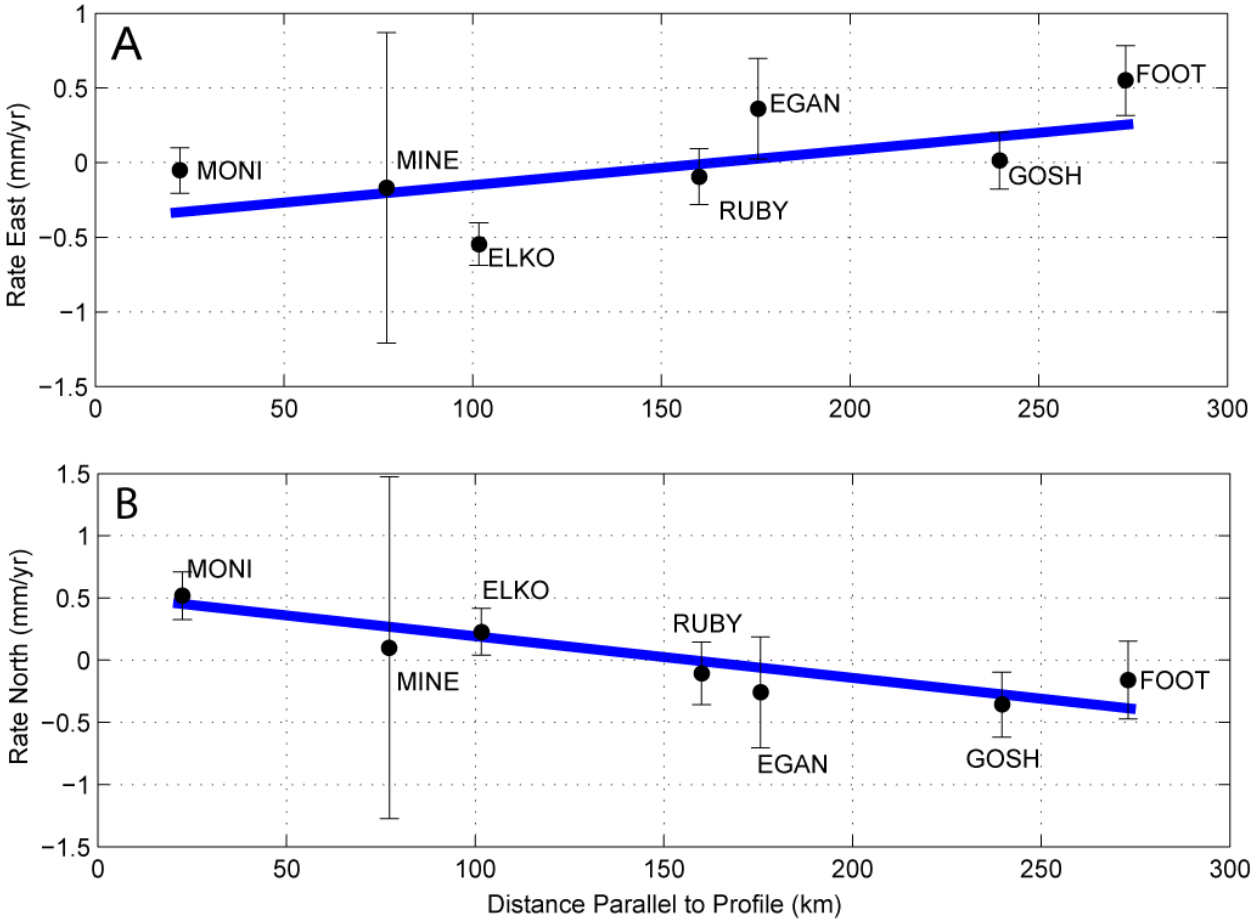

Figure 4. GPS rates for BARGEN permanent sites. A) East coordinate, B) North coordinate. Velocity gradients associated with the rigid-body motion of the Basin and Range near Wells have been estimated from the data and removed. Thus the gradients illustrated here are those resulting from deformation, and not solid body rotation. Error bars indicate 1-¤ uncertainty in rate.

As a result of the USGS program, a number of sites along U.S. Interstate Highway 80 and U.S. Highway 233 had been surveyed prior to the Wells earthquake, and were surveyed again after the event in order to constrain co-seismic displacement. The USGS resurveyed nine stations within approximately 70 km east and west of the epicenter. The USGS surveyed five of these stations in 1999 and 2003, three stations had been surveyed in 2003 and 2007, and the National Geodetic Survey had previously surveyed one station in 1994 and 1999. Unfortunately the station located closest to the epicenter (MOOR) apparently was destroyed sometime after 2003 when it was last surveyed by the USGS.

A minimum of 2 sessions 6.5 hours in length were collected at each monument with most stations recording 2-6 sessions 24 hours in length (table 2). The data were processed using JPL's GIPSY-OASIS II software using a modified precise positioning strategy (Zumberge and others, 1997). All data were processed using JPL precise orbit and clock files. The local data, including data from the 5-15 permanent stations that are in the same region, were processed together as a network to generate bias-fixed results. We then included the positions of approximately 30 globally distributed IGS stations. Using the positions from the global network, the local network is transformed into a North America fixed reference frame (Prescott and others, 2001). To mitigate the effect of common mode noise we used the positions of the permanent stations that were included in the solution to transform all position estimates into "regionally filtered" results following the approach of Hammond and Thatcher (2007). No permanent stations were present in 1994 so displacements were not calculated for station KEGG. The resulting time series from this processing can be found at: http://quake.wr.usgs.gov/research/deformation/gps/auto/Wells, and secular rates at these sites are shown in figure 6.

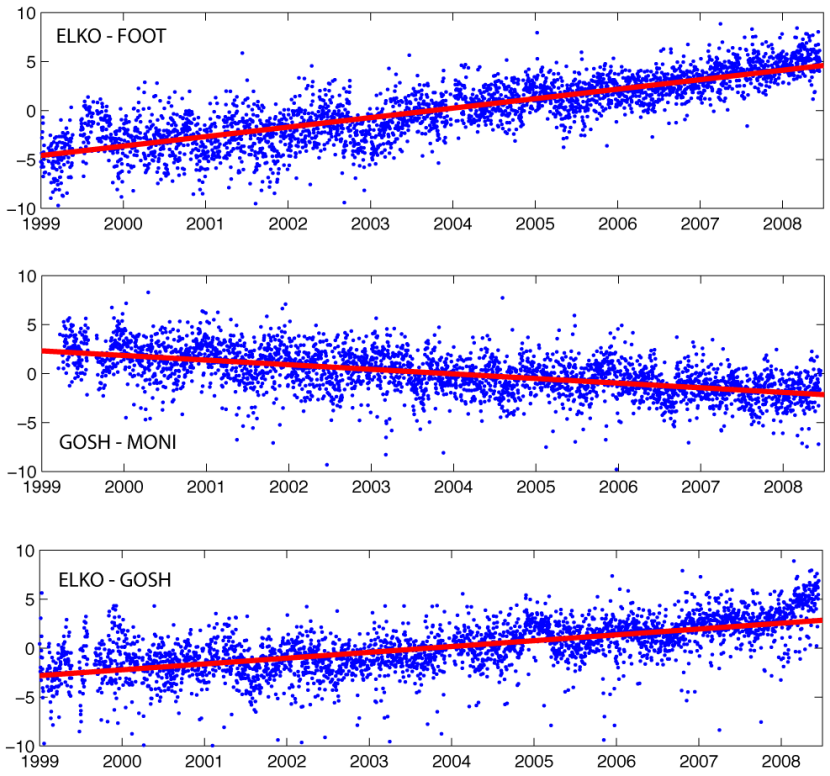

Figure 5. Line length changes between sites ELKO and FOOT, which got farther apart by approximately 10 mm over 10 years, GOSH and MONI which got closer to one another by approximately 5 mm, and ELKO and GOSH which got closer to one another by 5 mm. Vertical axis is the change in line length in mm. Red line is best-fitting straight line.

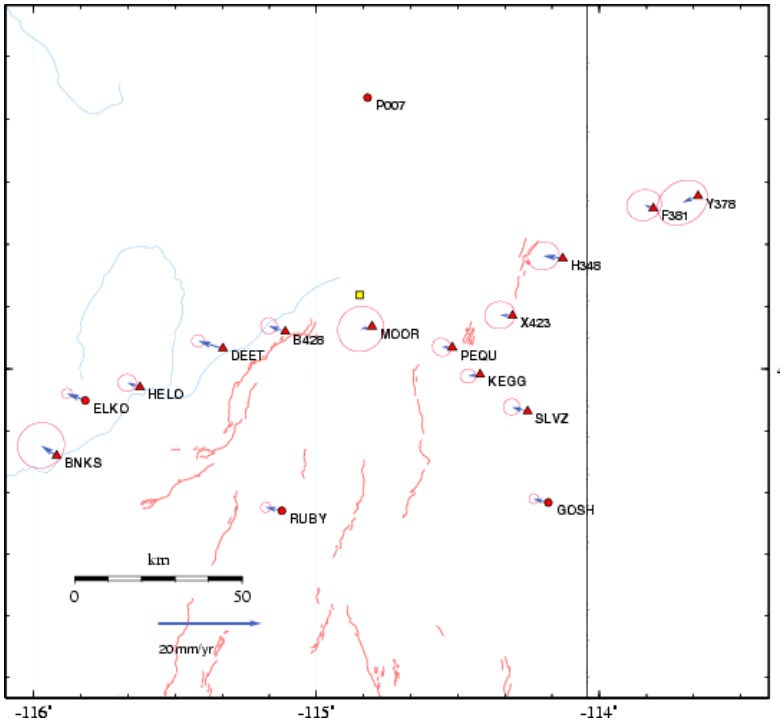

Figure 6. Secular GPS rates with respect to North America estimated at the USGS campaign sites, from USGS standard analysis (see text for URL reference). Note rate for site MOOR is available, but this GPS site was destroyed prior to the Wells earthquake. Red ellipses represent 95% confidence in rate estimates. Red lines are Quaternary fault traces.

Table 2. Wells region USGS campaign GPS site occupation history

Date Occupied	B428	DEET	F381	H348	HELO	KEGG	PEQU	SLVZ	X423
19940627						√			
19940629						√			
19990526						√			
19990527						√			
19990528						√			
19990915		√			√				
19990916	√	√							
19990917							√	√	
19990919		√			√				
19990920	√	√							
19990921							√	√	
20030620								√	
20030621	√								
20030623		√							
20030624	√						√		
20030625								√	
20030628					√				
20030703					√				
20030909			√	√					√
20030910			√						√
20030917				√					
20070906				√					√
20070907			√						√
20070912				√					
20070914			√						
20080224	√				√				√
20080225	√				√		√		√
20080226	√	√		√	√	√	√	√	√
20080227	√	√	√	√		√	√	√	√
20080228	√	√	√	√		√	√	√	√
20080229	√	√				√		√	√

Dates in yyyymmdd format.

Langbein (2004) presents a maximum likelihood method for fitting a time series employing a variety of temporal noise models. Using this approach we analyzed each station-component time series in order to estimate the secular rate, displacements at the time of the earthquake, and their standard errors. Although this method may be used to optimize the noise model parameters for permanent GPS time series, campaign GPS observations are not sufficiently frequent to do so. Therefore, we assume that the observations are contaminated by a combination of white, flicker, and random walk noise and fix the amplitudes of these processes to 2 mm, 1 mm/yr$^{1/4}$, and 2 mm/yr$^{1/2}$ respectively for the horizontal components and three times these values for the vertical. The resulting co-seismic displacement estimates for the campaign sites are given in table 3, and the co-seismic displacement field is shown in figure 7 (and also available at http://quake.wr.usgs.gov/research/deformation/gps/auto/Wells/Wells.cleaned/).

The secular rates with respect to stable North America are consistent with earlier results for these same benchmarks (figure 6; Hammond and Thatcher, 2005), but are more precise owing to the additional data collected in September 2007 and February 2008 (table 2). The co-seismic displacements, however, are larger than those expected from an elastic

dislocation model derived from the InSAR data (Amelung and Bell, 2008). In particular the sites DEET and PEQU have displacements greater than 16 mm in the east component that appear unlikely given the expectation based on the modeling of the InSAR and far-field permanent GPS sites. For both of these sites, the penultimate observation in the epoch preceding the earthquake consisted of only a single day of observation. Therefore the rates before the event were constrained only by the first observation set (surveyed in 1999) and a single day four years later (in June, 2003). Owing to a well-known effect in the fitting of a linear trend to sparse time series, this tends to underestimate the uncertainty in rate, since residual scatter around the later epoch is zero. If the InSAR and far field permanent GPS results are taken as true, then the misfit between observed and expected campaign GPS displacements provide an empirical estimate of the uncertainty in those displacements. Uncertainties for PEQU and DEET estimated this way are approximately 3 times the size of those listed in table 3. Except for the site HELO, the other campaign GPS sites have smaller discrepancies between the measured and expected displacements, but still require scaling by a factor of about 2 to explain the discrepancy with noise.

Since the uncertainty in rate before the event propagates into uncertainty in the estimate of co-seismic displacement, the value of these surveys would have been significantly enhanced if the surveys prior to the event had been more numerous and/or over a longer interval of time. Frequent surveying of the campaign benchmarks greatly improves resolution of long-term trends in crustal deformation patterns and is especially valuable in areas with long distances between regional permanent sites (e.g., in Nevada) in order to better estimate rates prior to an earthquake event. A benefit can also be obtained from future surveys of these sites, to better constrain the rate following the event.

Table 3. USGS Campaign GPS Site Co-seismic Displacements

				East (mm)		North (mm)		Up (mm)	
Station	**Longitude**	**Latitude**	**Monument type***	**Offset**	**1σ**	**Offset**	**1σ**	**Offset**	**1σ**
B428	-115.1100	41.0994	1	-4.5	2.1	2.4	2.0	13.5	22.6
DEET	-115.3310	41.0543	2	-16.7	2.6	8.5	2.6	43.3	24.3
F381	-113.8091	41.4297	1	1.13	1.2	4.4	1.2	13.1	7.8
H348	-114.1293	41.2957	2	5.3	1.1	0.1	1.1	8.2	7.4
HELO	-115.6244	40.9503	2	-0.1	2.1	11.3	2.1	14.4	22.6
PEQU	-114.5199	41.0577	2	16.6	2.7	-2.0	2.7	30.3	24.6
SLVZ	-114.2535	40.8855	2	-2.6	2.1	6.1	2.1	-38.7	22.7
X423	-114.3070	41.1425	3	2.2	1.0	-2.9	1.0	4.0	7.0

*** Monument type key:**
1 Rod driven to refusal
2 Disk set in concrete
3 Disk set in rock
Additional information on monuments can be found at: http://gpsstationinfo.wr.usgs.gov/

New Real Time GPS Monitoring in Wells, NV

Immediately following a significant earthquake there is an elevated probability that another, possibly larger event will occur. For this reason and because of the possible occurrence of postseismic ground deformations, on 28 April 2008 staff from the Nevada Seismological Laboratory (NSL) and Nevada Geodetic Laboratory (NGL) at the University of Nevada, Reno (UNR) installed a real-time telemetered GPS system. An earlier deployment of the GPS site was planned but not possible due to melting snow. This GPS site (named WLLS) is located at the southern end of the Snake Range, about 6 km north of the town of Wells, and is collocated with seismic instrumentation in order to share its data communication and power systems (figure 1, latitude 41.1669˚, longitude -114.9754˚). The location of WLLS is such that it reduces the maximum gap in the GPS network and thus provides better coverage for any future earthquake in this area.

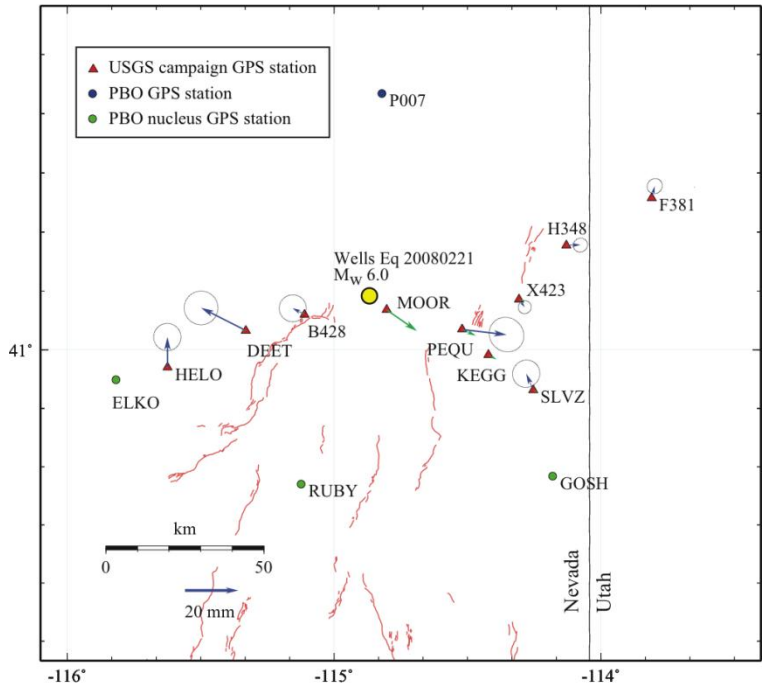

Figure 7. USGS Campaign GPS station co-seismic displacements measured after the Wells earthquake and 95% confidence uncertainties (blue). Predicted offsets using the model of Amelung and Bell, (2008) are too small to see at all sites except MOOR and PEQU (green vectors). Note that site MOOR was destroyed prior to the Wells earthquake. Estimates for co-seismic displacements at PBO sites are also too small to be visible. Red lines are traces of nearby Quaternary faults. Yellow circle indicates location of Wells earthquake.

The receiver collects data from the GPS satellites every 15 seconds and transmits the data directly to UNR for analysis. These high-rate samples are stored on the receiver for a few weeks after which they will be overwritten, unless they are transmitted to our laboratories for analysis (desirable in the case of a future event). At the end of every day the data are combined into a daily data file, which is transmitted automatically. The automated daily data retrieval allows for more rapid detection of motions that can indicate continued or new surface deformation since it is not necessary to visit the site to obtain data. WLLS uses a Trimble NetRS receiver and a zephyr geodetic antenna, and is otherwise identical to the existing 300-site semi-permanent "MAGNET" GPS network installed by UNR in the western Great Basin (Blewitt and others, 2009). Other than site WLLS, MAGNET sites are too far west of Wells to be useful for this study (see http://geodesy.unr.edu/networks). The monuments for MAGNET sites such as WLLS are in rock outcrops, and have been shown to produce position time series of comparable precision to those from permanent stations in the Basin and Range (Blewitt and others, 2009). A photograph of the environment surrounding the antenna is shown in figure 8, and its location is shown in figure 1.

Daily GPS data from WLLS has been processed and its time series of position in the GB1 reference frame has been generated from its date of installation to the time of this writing (25 October 2008). Time series from WLLS are shown in figure 9. With such a short time series it is difficult to assess postseismic deformation, especially since the size of the event was small compared to other events where significant postseismic deformations have been observed. Since no data were available from WLLS prior to the earthquake, it is not possible to evaluate whether the rate of crustal motion has changed subtly as a result of the earthquake. While small changes in slope of the east and up time series are visible just before 2008.6 (figure 9), these deflections are similar to the size of seasonal variations observed in other GPS time series in the Basin and Range (e.g., see figures 2 and 5). In the future, after a long time series has been collected (possibly years) it may be possible to detect very small changes in rate associated with transient deformations as they decay, if such processes are occurring.

Figure 8. Photograph of antenna for GPS site WLLS, which is now transmitting data daily to the Nevada Seismological Laboratory and Nevada Geodetic Laboratory, with the option of streaming high-rate data in real time. The location of this site is within 7 km of the epicenter and is shown in figure 1.

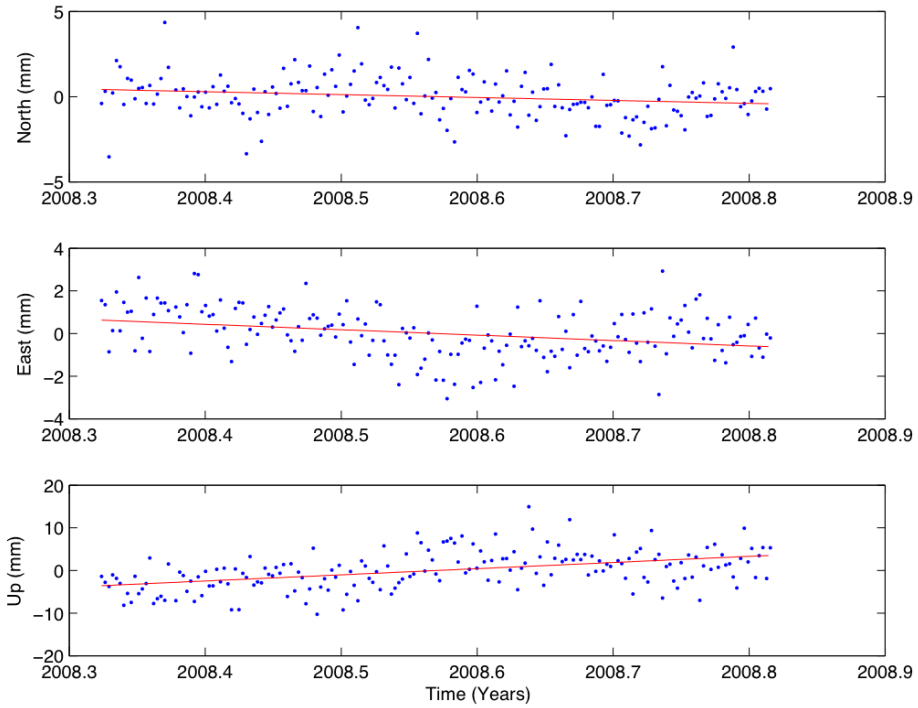

Figure 9. Time series from new GPS site WLLS in Wells, NV in GB1 reference frame. Red line is best-fitting straight line to data. Amount of scatter of position coordinates is similar to that for permanent site baselines shown in figure 5, indicating that the site is stable.

DISCUSSION

Our measurements of crustal strain contribute to a well-integrated picture of the seismic cycle and crustal deformation of eastern Nevada that is consistent with seismic and geologic data. For example, the azimuth of the direction of maximum horizontal crustal extension as measured by GPS (N59˚W) is very similar to the azimuth of co-seismic extension that occurred during the Wells earthquake (T-axis N60˚W, Harvard CMT, www. globalcmt.org). This suggests that the decade timescale preseismic strain accumulation determined by GPS represents loading of the crust in preparation for the earthquake. Furthermore, the orientation of the GPS-measured shear in the crust is aligned with the predominant direction of shear that is prevalent in the western Basin and Range, and San Andreas fault system (figure 3) and is consistent with this part of the Basin and Range behaving as an active component of the Pacific North/America plate boundary system. However, the N59˚W extension rate is approximately twice as large as the N31˚E contraction rate, indicating the state of deformation is transtensional, and possibility closer to uniaxial extension if the contraction is not significant.

Because we have estimates of the interseismic loading rate, and the amount of displacement that occurred in the earthquake, we can make some simple calculations that bear on seismic hazard in eastern Nevada. Assuming that the province is a simple 2D medium broken by normal faults every 30 km in the east west direction, 1 mm/yr of east-west extension over 250 km provides an estimate of 0.12 mm/yr average horizontal extension per fault system. This is consistent with the USGS Quaternary Fault and Fold Database classification of all faults in the area of <0.2 mm/yr (http://earthquake.usgs.gov/regional/qfaults/). If we assume that the fault on which the Wells event occurred is the location at this latitude where all of the extension is presently being accommodated, then a Wells-like event that slipped 0.5 meters on a plane dipping 40˚, must occur roughly every 3000 years to keep pace with the crustal extension. Thus events such as the Wells earthquake could occur every several thousand years, just about everywhere in the eastern Nevada Basin and Range if they are responsible for accommodating the extension that is measured with geodesy. However, they are not. The earthquake did not break the surface, so it has contributed zero displacement towards any cumulative extension of the crust of the type that would be measured by paleoseismic investigation. Furthermore, the earthquakes that have provided most of the moment release in the Basin and Range in historic time are larger (M 7, approximately) and less frequent (Pancha and others, 2006). They have slip magnitudes that are on the order of several meters (e.g., Slemmons, 1957; Wallace, 1984; Caskey and others, 1996) and thus would need to occur 2 to 10 times less frequently than the estimates for the M6 case, or approximately every 6000 to 30,000 years. This is consistent with recurrence intervals on other Basin and Range faults that have been dated paleoseismically (e.g., Caskey and others, 2000; Bell and others, 2004; Wesnousky and others, 2005). Thus the extension rate we measure geodetically is generally consistent with available paleoseismological slip rate and recurrence interval estimates, and the M6 Wells-type earthquake is probably not big enough to accommodate most of the extension of the Basin and Range.

The occurrence of the 21 February 2008 Wells, Nevada M 6.0 earthquake adds to the short list of normal faulting events in the Basin and Range that have been imaged geodetically. Furthermore it may be the only normal faulting earthquake to have been imaged both by ascending and descending InSAR and permanent GPS, making it possibly one of the best-observed normal faulting events on record, despite the fact that it occurred in one of the most remote areas in the western United States. Thus future seismic events will likely be even better constrained by geodetic measurements as the number of GPS sites grows and more InSAR data become available with shorter orbit repeat times and lower latency.

ACKNOWLEDGMENTS

We would like to thank the U.S. Geological Survey for their support of this study of the Wells, Nevada earthquake. We also thank UNAVCO Inc. for archiving and delivering data from the BARGEN and PBO permanent GPS networks. We thank the Nevada Bureau of Mines and Geology and the Nevada Seismological Laboratory for their support of the WLLS GPS station. GPS data analysis for this project was supported by the Department of Energy and Nevada System of Higher Education Cooperative Agreement DE-FC-04RW12232 for the Yucca Mountain Project, and by the NSF Tectonics and EarthScope programs under award numbers 0610031 and 0635757.

REFERENCES

Amelung, F., and Bell, J., 2008, InSAR Analysis of the 2008 Wells, Nevada earthquake [abs.]: EOS (Transactions of the American Geophysical Union), v. 89 no. 53, Fall Meeting Suppl., Abstract S51B-1745.

Bell, J. W., Caskey, S. J., Ramelli, A. R., and Guerrieri, L., 2004, Pattern and rates of faulting in the central Nevada seismic belt, and paleoseismic evidence for prior belt-like behavior: Bulletin of the Seismological Society of America, v. 94, no. 4, p. 1229–1254.

Bennett, R. A., Wernicke, B. P., Niemi, N. A., Friedrich, A. M., and Davis, J. L., 2003, Contemporary strain rates in the northern Basin and Range province from GPS data: Tectonics, v. 22, no. 1008, doi:10.1029/2001TC001355.

Blewitt, G., 2008, Fixed-Point theorems of GPS carrier phase ambiguity resolution and their application to massive network processing "Ambizap": Journal of Geophysical Research, v. 113, no. B12410, doi:10.1029/2008JB005736.

Blewitt, G., Hammond, W.C., and Kreemer, C., 2009, Geodetic constraints on contemporary deformation in the northern Walker Lane–1.Semi-permanent GPS strategy, *in* Oldow, J. S., and Cashman, P., editors, Late Cenozoic Structure and Evolution of the Great Basin–Sierra Nevada Transition, Geological Society of America Special Paper 447, p. 1–15, doi:10.1130/2009.2447(01).

Blewitt, G., and Lavalleé, D., 2002, Effect of annual signals on geodetic velocity: Journal of Geophysical Research, v. 107, no. B7, 2145, doi:10.1029/2001JB000570.

Caskey, J.S., Wesnousky, S.G., Zhang, P., and Slemmons, B.D., 1996, Surface faulting of the 1954 Fairview Peak (Ms=7.2) and Dixie Valley (Ms=6.9) earthquakes, central Nevada: Bulletin of the Seismological Society of America, v. 86, p. 761–787.

Caskey, J.S., Bell, J.W., Slemmons, B.D., and Ramelli, A.R., 2000, Historical surface faulting and paleoseismology of the central Nevada seismic belt, *in* Lageson, D.R., Peters, S.G., and Lahren, M.M., editors, Geological Society of America Field Guide 2, p. 23–44, Boulder, Colorado.

Chang, W.-L., Smith, R.B., and Meertens, C.M., 2006, Contemporary deformation of the Wasatch fault, Utah, from GPS measurements with implications for inter-seismic fault behavior and earthquake hazard—observations and kinematic analysis: Journal of Geophysical Research, v. 111, no. B11405, doi:10.1029/2006JB004326.

Davis, J.L., Bennett, R.A., and Wernicke, B.P., 2003, Assessment of GPS velocity accuracy for the Basin and Range Geodetic Network (BARGEN): Geophysical Research Letters, v. 30, p. 61–64.

Davis, J.L., Wernicke, B.P., Bisnath, S., Niemi, N.A., and Elosegui, P., 2006, Subcontinental-scale crustal velocity changes along the Pacific-North America plate boundary: Nature, v. 441, p. 1131–1134.

Dixon, T.H., Robaudo, S., Lee, J., and Reheis, M.C., 1995, Constraints on present-day Basin and Range deformation from space geodesy: Tectonics, v. 14, no. 4, p. 755–772.

Dixon, T.H., Miller, M., Farina, F., Wang, H., and Johnson, D., 2000, Present-day motion of the Sierra Nevada block and some tectonic implications for the Basin and Range Province, North American Cordillera: Tectonics, v. 19, no. 1, p. 1–24.

Dreger, D.S., Ford, S.R., and Ryder, I., *this volume*, Preliminary finite-source study of the February 21, 2008, Wells, Nevada Earthquake.

Hammond, W. C., 2004, Vertical motion of the Basin and Range, western United States from 10 Years of Campaign GPS *in* The state of GPS vertical positioning precision—separation of Earth processes by space geodesy: Cahiers du Centre Européen de Géodynamique et de Séismologie, Luxembourg.

Hammond, W. C., and Thatcher, W., 2004, Contemporary tectonic deformation of the Basin and Range province, western United States—10 years of observation with the Global Positioning System: Journal of Geophysical Research, v. 109, no. B08403, doi:10.1029/2003JB002746.

Hammond, W. C., and Thatcher, W., 2005, Northwest Basin and Range tectonic deformation observed with the Global Positioning System, 1999–2003: Journal of Geophysical Research, v. 110, no. B10405, doi:10.1029/2005JB003678.

Hammond, W. C., and Thatcher, W., 2007, Crustal deformation across the Sierra Nevada, Northern Walker Lane, Basin and Range transition, western United States measured with GPS, 2000-2004: Journal of Geophysical Research, v. 112, no. B05411, doi:10.1029/2006JB004625.

Henry, C., and Colgan, J., 2010, *this volume*, The regional structural setting of the 2008 Wells earthquake and Town Creek Flat basin—implications for the Wells earthquake fault and adjacent structures.

Koehler, R., and Wesnousky, S. G., 2010, Late Pleistocene regional extension rate derived from earthquake geology of late Quaternary faults across Great Basin, Nevada between 38.5˚ and 40˚ N latitude: Geological Society of America Bulletin, *in press*.

Kreemer, C., Blewitt, G., and Hammond, W. C., 2010, Evidence for an active shear zone in southern Nevada linking the Wasatch fault to the Eastern California Shear Zone: Geology, v. 38, no. 5, p. 475–476.

Langbein, J., 2004, Noise in two-color electronic distance meter measurements revisited: Journal of Geophysical Research, v. 109, no. B04406, doi:10.1029/2003JB002819.

Langbein J., 2008, Noise in GPS displacement measurements from Southern California and Southern Nevada: Journal of Geophysical Research, v. 113, no. B05405, doi:10.1029/2007JB005247.

Pancha, A., Anderson, J. G., and Kreemer, C., 2006, Comparison of seismic and geodetic scalar moment rates across the Basin and Range province: Bulletin of the Seismological Society of America, v. 96, no. 1, p. 11–32, doi:10.1785/0120040166.

Prescott, W. H., Savage, J. C., Svarc, J. L., and Manaker, D., 2001, Deformation across the Pacific-North America plate boundary near San Francisco, California: Journal of Geophysical Research, v. 106, no. 4, p. 6673–6682.

Puskas, C. M., Smith, R. B., Meertens, C. M., and Chang, W.-L., 2007, Crustal deformation of the Yellowstone-Snake River Plain volcano-tectonic system—campaign and continuous GPS observations, 1987–2004: Journal of Geophysical Research, v. 112, no. B03401, doi:10.1029/2006JB004325.

Savage, J. C., Lisowski, M., Svarc, J. L., and Gross, W. K., 1995, Strain accumulation across the central Nevada seismic zone, 1973–1994: Journal of Geophysical Research, v. 100 no. B10, p. 20,257–20,269.

Savage, J. C., Gan, W., and Svarc, J. L., 2001, Strain accumulation and rotation in the eastern California shear zone: Journal of Geophysical Research, v. 106, no. B10, p. 21,995–22,007.

Slemmons, B. D., 1957, Geological effects of the Dixie Valley-Fairview Peak, Nevada earthquakes of December 16, 1954: Bulletin of the Seismological Society of America, v. 47, p. 353–375.

Smith, K., Pechmann, J., Meremonte, M., Pankow, K., *this volume*, Preliminary analysis of the M_w 6.0 Wells, Nevada, earthquake sequence.

Svarc, J. L., Savage, J. C., Prescott, W. H., and Ramelli, A. R., 2002, Strain accumulation and rotation in western Nevada, 1993-2000: Journal of Geophysical Research, v. 107, no. B5, 10.1029/2001JB000579.

Thatcher, W., Foulger, G. R., Julian, B. R., Svarc, J. L., Quilty, E., and Bawden, G. W., 1999, Present-day deformation across the Basin and Range province, western United States: Science, v. 283, p. 1714–1718.

Wallace, R. E., 1984, Faulting related to the 1915 earthquakes in Pleasant Valley, Nevada: U.S. Geological Survey Professional Paper, v. 1274-A, B, p. A1–A33.

Wdowinski, S., Bock, Y., Zhang, J., Fang, P., and Genrich, J., 1997, Southern California permanent GPS geodetic array— spatial filtering of daily positions for estimating co-seismic and postseismic displacements induced by the 1992 Landers earthquake: Journal of Geophysical Research, v. 102, no. B8, p. 18,057–18,070.

Wernicke, B. P., Friedrich, A. M., Niemi, N. A., Bennett, R. A., and Davis, J. L., 2000, Dynamics of plate boundary fault systems from Basin and Range Geodetic Network (BARGEN) and Geologic Data: GSA Today, v. 10, no. 11, p. 1–7.

Wernicke, B., Davis, J. L., Niemi, N. A., Luffi, P., and Bisnath, S., 2008, Active megadetachment beneath the western United States: Journal of Geophysical Research, v. 113, no. B11409, doi:10.1029/2007JB005375.

Wesnousky, S. G., Baron, A. D., Briggs, R. W., Caskey, J. S., Kumar, S. J., and Owen, L., 2005, Paleoseismic transect across the northern Great Basin: Journal of Geophysical Research, v, 110, no. B05408, doi:10.1029/2004JB003283.

Zumberge, J. F., Heflin, M. B., Jefferson, D. C., Watkins, M. M., and Webb, F. H., 1997, Precise point positioning for the efficient and robust analysis of GPS data from large networks: Journal of Geophysical Research, v. 102, no. B3, p. 5005–5017.